Ultimate bearing capacity at the tip of a pile in rock based on the modified Hoek–Brown criterion

A. Serrano, C. Olalla, R.A Galindo

1. Introduction

A method for calculating the ultimate bearing capacity at the tip of a pile that is embedded in rock, according to the theory of plasticity, was presented in a previous paper [1] using the original Hoek–Brown failure criterion [2]. Hoek et al. [3] modified their original model, in order to apply it to highly fractured media (RMR ≤ 25), incorporating a new exponent "a" ranging between 0.5 and 0.65. A value of the exponent of $a=0.5$ corresponds to the original criterion.

In this technical note, the method for obtaining the ultimate bearing capacity is generalized for the modified Hoek–Brown criterion. All the hypotheses, and thus the validity and applicability of the new method, are the same as the old one: perfect plasticity theory, weightless mass, without inertia forces, Meyerhof's hypothesis [4], De Beer shape factor [5], etc. Consequently, this paper should be read together with the previous one [1].

New expressions, in order to discriminate between the four possible cases, according to the values of the overburden pressure and the embedment ratio, are obtained for different magnitudes of exponent a, which allow the ultimate bearing capacities to be calculated. For an exponent $a=0.5$ the results obtained match with the original Hoek–Brown failure criterion.

The ultimate bearing capacity of the pile is assumed to be only derived from toe resistance. This assumption is obviously on the safety side. If the contribution of shaft resistance should be incorporated, considerations must be given to the load transfer behavior of the pile-socket system. The magnitude of the shaft resistance could be analyzed as independent and engineering judgment must argue with caution both contributions.

2. The modified Hoek–Brown failure criterion

The modified Hoek–Brown criterion [3], which is particularly suitable for extremely fractured rock mass, reads as follows:

$$\frac{\sigma_1-\sigma_3}{\sigma_c}=\left(m\frac{\sigma_3}{\sigma_c}+s\right)^a \tag{1}$$

where σ_1 is the major principal stress at failure, σ_3 is the minor principal stress, σ_c is the uniaxial compressive strength of the matrix rock, and m, s are constants that depend on the characteristics of the rock mass and its degree of fracturing [6]. The value of the exponent a also depends in a generalized form on the degree of fracturing by means of the Geological Strength Index (GSI) [6]

$$a=\frac{1}{2}+\frac{1}{6}(e^{-GSI/15}-e^{-20/3}) \tag{2}$$

Analyzing deep foundation problems the disturbance factor D must be assumed always to be $D=0$. Fig. 1 shows the exponent of Eq. (2) which is compared with previous expressions.

The expression for the modified Hoek–Brown failure criterion involving Lambe's variables for plane strain analysis, ($p=(\sigma_1+\sigma_3)/2$ and $q=(\sigma_1-\sigma_3)/2$), allows for a simplified and normalized treatment of the rock mass failure phenomenon. With these variables, the modified Hoek–Brown failure criterion is expressed as follows [7]:

$$\frac{p}{\beta_a}+\zeta_a=\left[1+(1-a)\left(\frac{q}{\beta_a}\right)^k\right]\frac{q}{\beta_a} \tag{3}$$

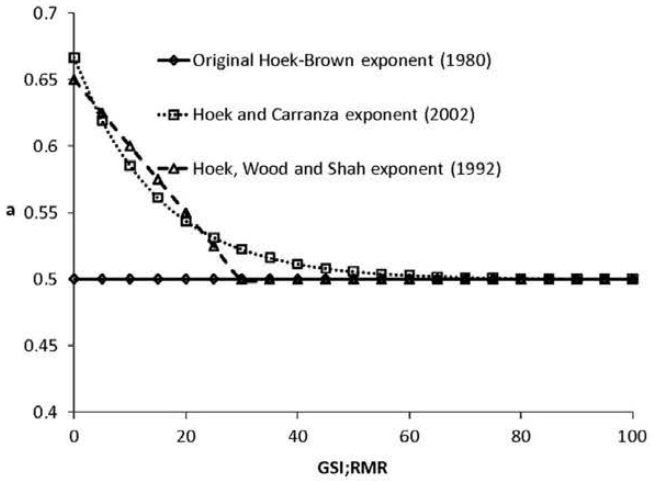

Fig. 1. Variation of the exponent with the degree of fracturing.

where k, β_a and ζ_a are constants for the rock mass, and depend on a, m, s and σ_c in the following way:

$$k=(1-a)/a;\ \beta_a=A_a\sigma_c;\ \zeta_a=s/(mA_a)$$

$$A_a=(m(1-a)/2^{1/a})^{1/k} \tag{4}$$

In dimensionless and normalized form, Eq. (3) becomes

$$p_0^*\equiv p^*+\zeta_a=[1+(1-a)q^{*k}]q^* \tag{5}$$

where p^* and q^* are the normalized and dimensionless Lambe's variables, ($p_0^*=p/\beta_a+\zeta_a$; $q^*=q/\beta_a$). *Note*: in this paper when the asterisk is present it means that stresses are non-dimensional.

The envelope of Mohr failure circles, $\tau=\tau(\sigma)$, is defined by

$$\tau=q\ \cos\ \rho \tag{6}$$

$$\sigma=p-q\ \sin\ \rho \tag{7}$$

where ρ is the "instantaneous friction angle". This is the angle that the tangent to the Mohr–Coulomb envelope forms with the abscissa axis, at the tangent point to Mohr's circle.

The following equation is obtained using previous expressions [8]:

$$\frac{\mathrm{d}q}{\mathrm{d}p}=\ \sin\ \rho \tag{8}$$

Taking into account Eq. (5)

$$\sin\ \rho=\frac{\mathrm{d}q^*}{\mathrm{d}p_0^*}=\frac{1}{1+kq^{*k}} \tag{9}$$

The following parametric equations are obtained for the criterion with Lambe's variables [after (5) and (9)]:

$$q^*\equiv\frac{q}{\beta_a}=\left[\frac{1-\ \sin\ \rho}{k\ \sin\ \rho}\right]^{1/k} \tag{10}$$

$$p_0^*\equiv\frac{p}{\beta_a}+\zeta_a=a\left[\frac{1+k\ \sin\ \rho}{\sin\ \rho}\right]\left[\frac{1-\ \sin\ \rho}{k\ \sin\ \rho}\right]^{1/k} \tag{11}$$

The parametric expressions for Mohr's envelope, for the generalized Hoek–Brown failure criterion (2002) under associative flow law, can be obtained by taking into account (6), (7) and (10), (11)

$$\tau^*\equiv\frac{\tau}{\beta_a}=\left[\frac{1-\ \sin\ \rho}{k\ \sin\ \rho}\right]^{1/k}\ \cos\ \rho \tag{12}$$

$$\sigma_0^*\equiv\frac{\sigma}{\beta_a}+\zeta_a=(a+\ \sin\ \rho)\left[\frac{1-\ \sin\ \rho}{\sin\ \rho}\right]\left[\frac{1-\ \sin\ \rho}{k\ \sin\ \rho}\right]^{1/k} \tag{13}$$

They represent the key expressions of all this mathematical process. From a mathematical point of view they are completely rigorous.

3. Obtaining Riemann's invariant

When there are no mass forces along the characteristic stress lines, the following differential equations are verified [8], where ψ is the angle that forms the major principal stress (σ_1) with the vertical axis

$$\frac{\cos\ \rho}{2q}\mathrm{d}p\pm\mathrm{d}\psi=0 \tag{14}$$

If Eq. (8) is taken into account, together with Eqs. (10) and (11), then

$$\frac{\cot\rho}{2}\frac{\mathrm{d}q}{q}\pm\mathrm{d}\psi=0 \tag{15}$$

Taking into account Eq. (10)

$$\frac{\mathrm{d}q}{q}=\frac{1+\ \sin\ \rho}{k\ \sin\ \rho\ \cos\ \rho} \tag{16}$$

The "Riemann's invariant" $I_a(\rho)$ is

$$I_a(\rho)\equiv\int\mathrm{d}I_a(\rho)=\int\frac{\cos\ \rho}{2q}\mathrm{d}p=\int\frac{\cot\rho}{2}\frac{\mathrm{d}q}{q} \tag{17}$$

Taking into account Eq. (16)

$$\int\mathrm{d}I_a(\rho)=-\frac{1}{k}\int\frac{1+\ \sin\ \rho}{2\sin^2\rho}\mathrm{d}p \tag{18}$$

The change of the Riemann's invariant along the characteristic stress lines represents the change of position of the pole on Mohr's circles, as Eq. (15) expresses. The Riemann's invariant is useful because, if the change of the position of the pole is known, evaluates the change of the instantaneous friction angle (known from the Riemann's invariant), and then Mohr's circle which allows the evaluation of the stresses is obtained.

The invariant for the modified Hoek–Brown criterion is obtained integrating Eq. (18) [7]:

$$I_a(\rho)=\frac{1}{2k}\left[\cot\rho+\ln\left(\cot\left(\frac{\rho}{2}\right)\right)\right] \tag{19}$$

4. Ultimate bearing capacity

4.1. Procedure

The general plasticity theory of the ultimate bearing capacity theory is applied to a specific case assuming that the modified Hoek–Brown criterion applies. The used methodology is identical to the one used in previous papers [1,7,8].

Along the characteristic lines, the following is verified if there is no ground weight:

$$\mathrm{d}I_a(\rho)\pm\mathrm{d}\psi=0 \tag{20}$$

If this expression is integrated between one point lying on Boundary 1 and another point lying on Boundary 2, the following

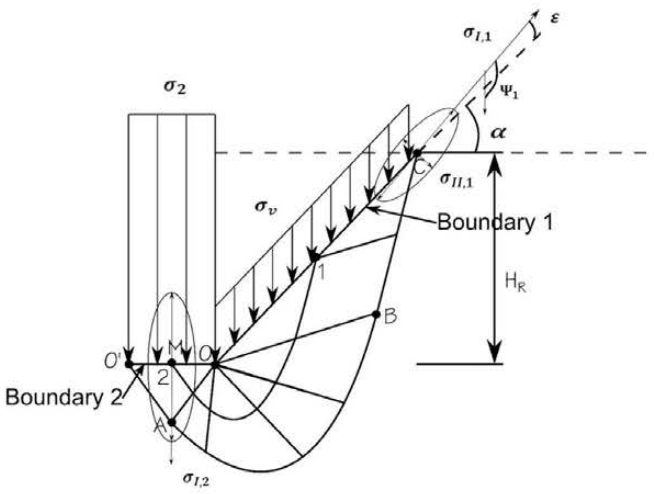

Fig. 2. Sketch of assumed failure.

holds (see Fig. 2):

$$I_a(\rho_1) \pm \psi_1 = I_a(\rho_2) \pm \psi_2 \tag{21}$$

This expression is the key to finding the ultimate bearing capacity. If the values of variables ψ_1 and ρ_1 at Boundary 1 and variable ψ_2 under the pile (Boundary 2) are known, then ρ_2 can be obtained. This friction angle ρ_2 makes it possible to determine the ultimate bearing capacity by means of Eq. (13).

Firstly, the ultimate bearing capacity under the plane strain hypotheses is obtained when the overburden pressure is h_m and the embedment ratio is n. Subsequently, the ultimate bearing capacity of the pile is obtained by multiplying it by the shape factor s_β defined by De Beer [5]. It depends only on one friction angle (Mohr's Coulomb theory) and in this case it is assumed to be a function of the average instantaneous angle of friction (ρ_m), which is then established through ρ_1 and ρ_2.

4.2. Boundary conditions

In the case of the ultimate bearing capacity, the so-called maximum and minimum Mohr's circles refer to stress conditions at Boundaries 1 and 2, respectively.

4.2.1. Boundary 1

The vertical stress σ_v exerted upon the middle point of Boundary 1 is

$$\sigma_v^* = h_m \cos \alpha \tag{22}$$

$$h_m = \frac{H_R \gamma_R}{2\beta_a} + \frac{H_s \gamma_s}{\beta_a} \tag{23}$$

where the overburden pressure h_m depends on the rock weight $H_R\gamma_R$ and the ground weight $H_s\gamma_s$ exerted on the rock surface, and α is the angle of the ascending exterior surface (Boundary 1).

The normal (σ) and shear (τ) components acting at the plane that represents Boundary 1 are as follows:

$$s_1^* = \frac{\sigma}{\beta_a} + \zeta_a = h_m \cos^2 \alpha \tag{24}$$

$$t_1^* = \frac{\tau}{\beta_a} = h_m \cos \alpha \sin \alpha \tag{25}$$

In a diagram τ, σ, the stresses acting upon Boundary 1 are located on a circle whose diameter is h_m; which will be referred to as the "overburden circle".

It can be demonstrated [1] that as far as the Hoek and Brown strength criterion is concerned, there could be two types of overburden pressures, depending on whether h_m is greater or smaller than the unconfined compressive strength σ_{cm} of the rock mass expressed in dimensionless form $(2(\zeta_a/(1-a))^a)$:

- Circles for small overburden pressure $h_m < 2(\zeta_a/1-a)^a$
- Circles for great overburden pressure $h_m > 2(\zeta_a/1-a)^a$

Bearing in mind that shear and normal stresses at Boundary 1 are known (τ_1 and σ_1), then the instantaneous friction angle (ρ_1) is directly obtained by the equation that defines Mohr's stresses circle

$$(t_1^*)^2 + (p_1^* - s_1^*)^2 = (q_1^*)^2 \tag{26}$$

This equation, together with Eqs. (24) and (25) allows to express the angle α in the following way:

$$\cos^2 \alpha = \frac{(p_1^*)^2 - (q_1^*)^2}{2p_1^* h_m - h_m^2} \tag{27}$$

This equation links the angle of virtual inclination (α) with the overburden pressure h_m and with the instantaneous angle of friction for Boundary 1 (ρ_1), according to Hoek and Brown's parametric strength law, Eqs. (10) and (11). For a given value of h_m; if α is known, it is possible to determine ρ_1.

The inclination of the major principal stress, (ψ_1), at Boundary 1 is expressed by the following [1,7]:

$$\psi_1 = \frac{\pi}{2} + \alpha + \varepsilon \tag{28}$$

The angle ε is given by

$$\tan 2\varepsilon = \frac{t_1^*}{p_1^* - s_1^*} \tag{29}$$

Therefore, the equation to obtain the inclination of the major principal stress inclinations at Boundary 1 is a function of the instantaneous friction angle ρ_1.

4.2.2. Transmission from Boundary 1 to Boundary 2

The value of $I_a(\rho_2)+\psi_2$ in Boundary 2 can be found using Riemann's modified invariant

$$I_a(\rho_1) + \psi_1 = I_a(\rho_2) + \psi_2 \tag{30}$$

The inclination of the main major stress at Boundary 2, (ψ_2), is zero; due to the fact that the pile tip load is always vertical. The preceding equation allows ρ_2 to be obtained through the inverse function of Riemann's Invariant (I_a^{-1}):

$$\rho_2 = I_a^{-1}[I_a(\rho_1) + \psi_1] \tag{31}$$

4.2.3. Boundary 2

Once the instantaneous friction angle for Boundary 2 (ρ_2) is known, Lambe's variables that define Mohr's circle (p_2, q_2) can be obtained by expressions (10) and (11). The dimensionless vertical stress exerted upon Boundary 2, σ_2^*, is the major principal stress, because $\psi_2 = 0$. Therefore, the vertical stress with pressure dimensions, σ_2, the ultimate bearing capacity that is the purpose of the

calculations for the entire process considering plane strain, is

$$\sigma_2 \equiv \beta_a \sigma_2^* = \beta_a (N_\beta - \zeta_a) \tag{32}$$

where

$$N_\beta = \left[\frac{1-\sin\rho_2}{k\sin\rho_2}\right]^{1/k} + a\left[\frac{1+k\sin\rho_2}{\sin\rho_2}\right]\left[\frac{1-\sin\rho_2}{k\sin\rho_2}\right]^{1/k} \tag{33}$$

4.2.4. The embedment ratio

The embedment ratio ($n = H_R/B$, being B the pile diameter) can be obtained from the equation that defines the characteristic line O'ABC (Fig. 2). It determines the limits of the plastified zone. Thus, in Prandtl's plastified radial zone, the following holds [5]:

$$\frac{OB}{OA} = \sqrt{\frac{q_2\cos\rho_2}{q_1\cos\rho_1}} \tag{34}$$

Applying Eqs. (10) and (11) this relationship can be expressed as a function of the instantaneous friction angles in both boundaries. In the straight sections of the characteristic line corresponding to the plastified zone, the result by applying the law of sines in triangles OBC and OMA is obtained. The ratio of embedment is a generalized expression presented in paper [1]

$$n = \sin\alpha \frac{\cos\mu_1}{\sin(\mu_1+\varepsilon)} \frac{\sin\mu_1}{\sin\mu_2} \sqrt{\frac{\cos\rho_2}{\cos\rho_1}\left[\left(\frac{1-\sin\rho_2}{1-\sin\rho_1}\right)\left(\frac{\sin\rho_1}{\sin\rho_2}\right)\right]^{1/k}} \tag{35}$$

where μ_1 and μ_2 are the directions of the two families of characteristic lines, respectively:

$$\mu_1 = \frac{\pi}{4} - \frac{\rho_1}{2};\ \mu_2 = \frac{\pi}{4} - \frac{\rho_2}{2}$$

In the case of the major overburden circles, the limiting state n_{L1} occurs when Mohr's circle for Boundary 1 is tangent to Mohr's envelope at the point where the latter cuts the overburden circle (stresses t_{L1} and s_{L1}). Consequently, the following is verified at this point:

$$h_m = \frac{(t_{L1}^*)^2 + (s_{L1}^*)^2}{s_{L1}^*} = H(\rho_{L1}) \tag{36}$$

Therefore, h_m is a function of the limit friction angle ρ_{L1} and then it is obtained as $\rho_{L1} = H^{-1}(h_m)$.

For its part, the angle α_{L1} can be calculated by means of the following equation:

$$\tan\alpha_{L1} = \frac{q_{L1}^*\cos\rho_{L1}}{p_{L1}^* - q_{L1}^*\sin\rho_{L1}} \tag{37}$$

Therefore, it is obtained as:

$$n_{L1} = \frac{\sin\alpha_{L1}}{2\sin\mu_2}\sqrt{\frac{\cos\rho_2}{\cos\rho_{L1}}\left[\left(\frac{1-\sin\rho_2}{1-\sin\rho_{L1}}\right)\left(\frac{\sin\rho_{L1}}{\sin\rho_2}\right)\right]^{1/k}} \tag{38}$$

In the case of the minor overburden circle, the limiting embedment condition n_{L2} is reached when Mohr's circle for Boundary 1 stress coincides with Mohr's circle for the unconfined compressive strength conditions. Under these circumstances

$$p_{L2}^* = q_{L2}^* = \left(\frac{\zeta_a}{1-a}\right)^a$$
$$\sin\rho_{L2} = \frac{1}{1+k(q_{L2}^*)^k}$$
$$\mu_{L2} = \frac{\pi}{4} - \frac{\rho_{L2}}{2}$$
$$\alpha_{L2} = \frac{\pi}{2}$$

Thus, the following equation is obtained:

$$n_{L2} = \frac{\cos\mu_{L2}}{\sin\mu_2}\sqrt{\frac{\cos\rho_2}{\cos\rho_{L2}}\left[\left(\frac{1-\sin\rho_2}{1-\sin\rho_{L2}}\right)\left(\frac{\sin\rho_{L2}}{\sin\rho_2}\right)\right]^{1/k}} \tag{39}$$

Fig. 3 shows the limiting embedment n_{L1} and n_{L2} together for different values of exponent a (a=0.55 in (a); a=0.60 in (b); a=0.65 in (c).

4.2.5. Shape coefficient

Once the ultimate bearing capacity has been obtained under the plane strain hypothesis, it is necessary to take into account the real three-dimensional geometry of the pile. A shape coefficient s_β must be applied. The formulation developed by De Beer [5] is as follows: $s_\beta = 1 + \tan\rho_m$, where ρ_m is an average angle of friction and is considered to be the most appropriate among other possibilities.

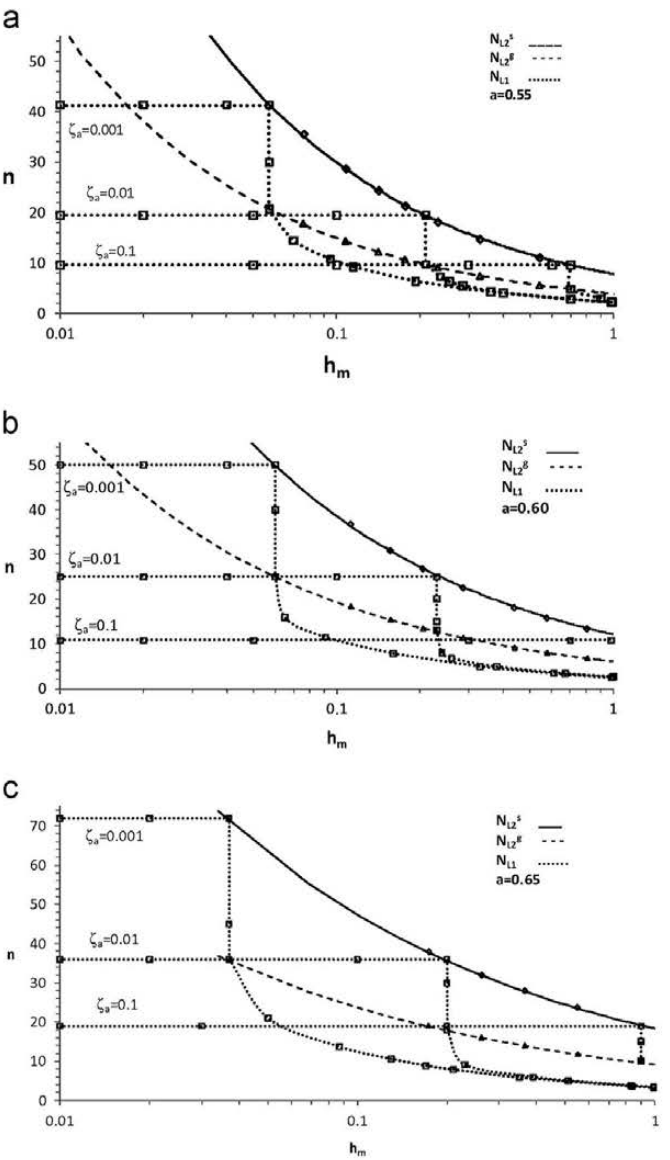

Fig. 3. (a) Limit values for the embedment ratio n as a function of the overburden pressure h_m for different values of parameter ζ_a. Value of the exponent a=0.55. (b) Limit values for the embedment ratio n as a function of the overburden pressure h_m for different values of parameter ζ_a. Value of the exponent a=0.60. (c) Limit values for the embedment ratio n as a function of the overburden pressure h_m for different values of parameter ζ_a. Value of the exponent a=0.65.

As defined in the previous paper [1], it is possible to calculate the average angle of friction by the expression

$$\rho_m = a \sin\left(\frac{q_2 - q_1}{p_2 - p_1}\right) \tag{40}$$

Substituting Eqs. (10) and (11) in Eq. (40), the value ρ_m function of the instantaneous friction angles in both boundaries is obtained. The ultimate bearing capacity at the tip of a pile (σ_{hp}), once the dimensionless factor has been included, is

$$\sigma_{hp} = \sigma_2 s_\beta = \beta_a (N_\beta - \zeta_a) s_\beta = \beta_a N_{\beta p} \tag{41}$$

5. Examples

The ultimate bearing capacity at the tip of a pile is calculated using the following data: $GSI(\approx RMR) = 15$; $m_0 = 15$; $\sigma_c = 5$ MPa; $\gamma_R = 15$ kN/m^3; $B = 0.8$ m; $H_s = 6$ m; $\gamma_s = 18$ kN/m^3.

Case 1. The pile is embedded in rock to a depth of $H_R = 0.8$ m.

(A) Hoek–Brown parameters:

$$m = m_0 e^{((GSI-100)/28)} = 0.7206$$

$$s = e^{((GSI-100)/9)} = 7.913 \times 10^{-5}$$

$$a = \frac{1}{2} + \frac{1}{6}(e^{-GSI/15} - e^{-20/3}) = 0.56$$

(B) Intermediate parameters:

$$k = \frac{1-a}{a} = 0.783$$

$$A_a^k = m(1-a)/2^{1/a} = 0.092$$

$$A_a = 0.092^{1/0.783} = 0.0475$$

$$\beta_a = A_a \sigma_c = 0.237 \text{ MPa}$$

$$\zeta_a = \frac{s}{m A_a} = 0.0023$$

(C) Iteration procedure:
Using Fig. 4 (deduced from Fig. 3), the type of pile behavior to consider for the calculation can be obtained. In this case

$$h_m = \frac{H_R \gamma_R}{2\beta_a} + \frac{H_s \gamma_s}{\beta_a} = 0.481$$

$$n = \frac{H_R}{B} = 1$$

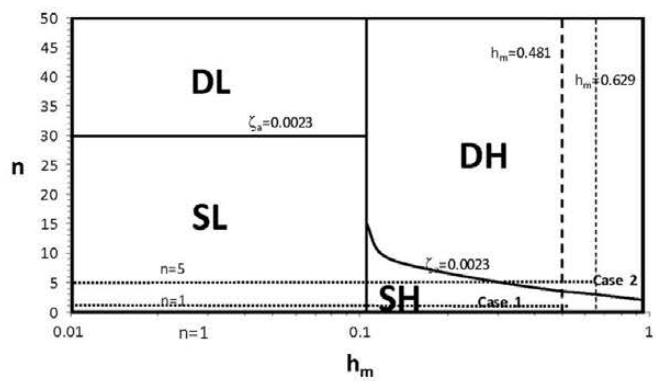

Fig. 4. Different pile types ($\zeta_a = 0.0023$) as a function of the embedment ratio (n) and the overburden pressure. Value of the exponent $a = 0.56$.

Therefore, it is a semi-deep pile with large overburden (SH). Increasing values of angle α are used in the process. For each value of the angle α, instantaneous friction angle in boundary 1, ρ_1, is obtained by means of Eq. (27) and friction angle in boundary 2, ρ_2, is calculated using Eq. (31). The value of α achieved is iterated until when Eq. (35) is satisfied. In this case, the following values are obtained:

$$\alpha = 17.8^\circ$$

$$\rho_1 = 35.2^\circ$$

$$\rho_2 = 15.4^\circ$$

$$\rho_m = 20.8^\circ$$

(D) Ultimate bearing capacity:

$$s_\beta = 1 + \tan \rho_m = 1.38$$

$$N_\beta = \left[\frac{1 - \sin\rho_2}{k \sin\rho_2}\right]^{1/k} + a\left[\frac{1 + k \sin\rho_2}{\sin\rho_2}\right]\left[\frac{1 - \sin\rho_2}{k \sin\rho_2}\right]^{1/k} = 17.98$$

$$N_{\beta p} = (N_\beta - \zeta_a) s_\beta = 24.80$$

$$\sigma_{hp} = \beta_a N_{\beta p} = 5.88 \text{ MPa}$$

Case 2. The same pile is embedded in rock to a depth of $H_R = 4$ m.

The Hoek–Brown parameters (A) and the intermediate parameters (B) are the same as those calculated in Case 1.

(A) Iteration procedure:
From Fig. 4 (obtained from Fig. 3), the type of pile to consider for the calculation is a deep pile and large overburden (DH). Increasing values of angle α are used in the process. For each value of the angle α, instantaneous friction angle in boundary 1, ρ_1, is obtained by means of Eq. (27) and friction angle in boundary 2, ρ_2, is calculated using Eq. (31). The value of α is iterated until the value of n_{L1} calculated with Eq. (38) allows to obtain a h_m that satisfies Eq. (27). In this case (DH), a value of $h_m = 0.629$ is obtained. In this case, the following values are achieved:

$$\alpha = 54.1^\circ$$

$$\rho_1 = 44.7^\circ$$

$$\rho_2 = 13.2^\circ$$

$$\rho_m = 19.5^\circ$$

(B) Ultimate bearing capacity:

$$s_\beta = 1 + \tan \rho_m = 1.35$$

$$N_\beta = \left[\frac{1 - \sin\rho_2}{k \sin\rho_2}\right]^{1/k} + a\left[\frac{1 + k \sin\rho_2}{\sin\rho_2}\right]\left[\frac{1 - \sin\rho_2}{k \sin\rho_2}\right]^{1/k} = 25.06$$

$$N_{\beta p} = (N_\beta - \zeta_a) s_\beta = 33.83$$

$$\sigma_{hp} = \beta_a N_{\beta p} = 8.02 \text{ MPa}$$

6. Numerical model

In this section, a numerical model to calculate the ultimate bearing capacity at the tip of a pile is shown, using the

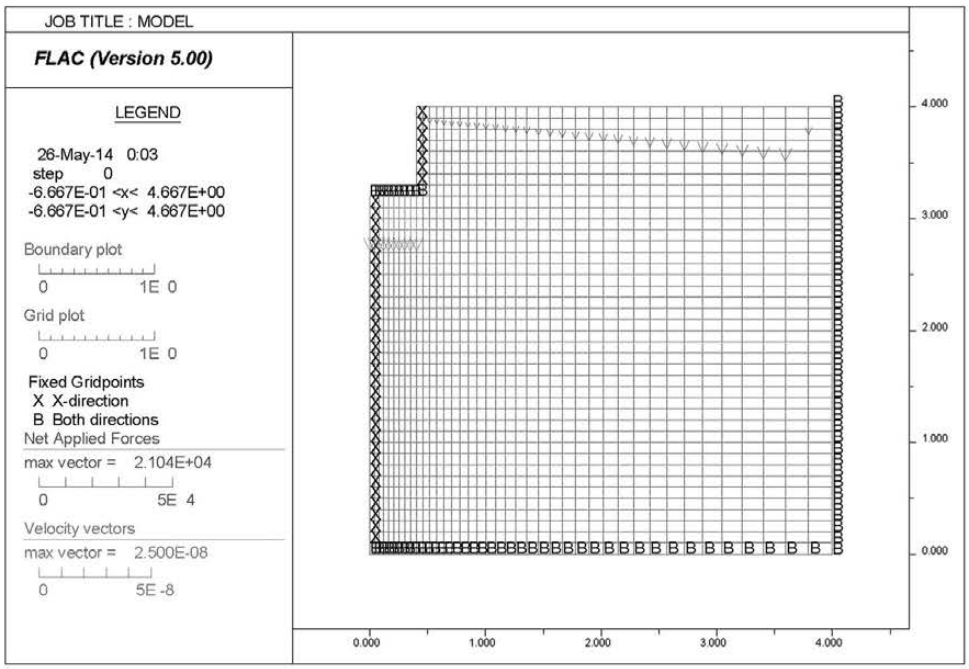

Fig. 5. Numerical model for calculating the ultimate bearing capacity at the tip of a pile that is embedded in rock.

Table 1
Ultimate bearing capacity results obtained by analytical solution and numerical solution, being $GSI=15$; $\gamma_R=15$ kN/m^3; $B=0.8$ m; $H_s=6$ m; $\gamma_s=18$ kN/m^3.

Ultimate bearing capacity at the tip (MPa)	$H_R=0.8$ m, $\sigma_c=5$, $m_0=15$	$H_R=0.8$ m, $\sigma_c=5$, $m_0=7$	$H_R=0.8$ m, $\sigma_c=2$, $m_0=15$	$H_R=4$ m, $\sigma_c=5$, $m_0=15$	$H_R=4$ m, $\sigma_c=5$, $m_0=7$	$H_R=4$ m, $\sigma_c=2$, $m_0=15$
2D analytical solution: (a_A)	4.3 MPa	2.4 MPa	2.5 MPa	5.9 MPa	3.0 MPa	3.1 MPa
2D numerical solution: (a_N)	4.6 MPa	2.5 MPa	2.6 MPa	6.5 MPa	3.4 MPa	3.5 MPa
Error: $((a_A)-(a_N))/(a_N)$	0.065	0.040	0.038	0.092	0.117	0.114
De Beer's factor: (f)	1.38	1.31	1.32	1.35	1.30	1.30
3D proposed solution: $(b_A)=(a_A)*(f)$	5.9 MPa	3.2 MPa	3.3 MPa	8.0 MPa	3.9 MPa	4.0 MPa
3D numerical solution (b_N)	9.0 MPa	5.0 MPa	5.7 MPa	11.2 MPa	5.5 MPa	6.5 MPa

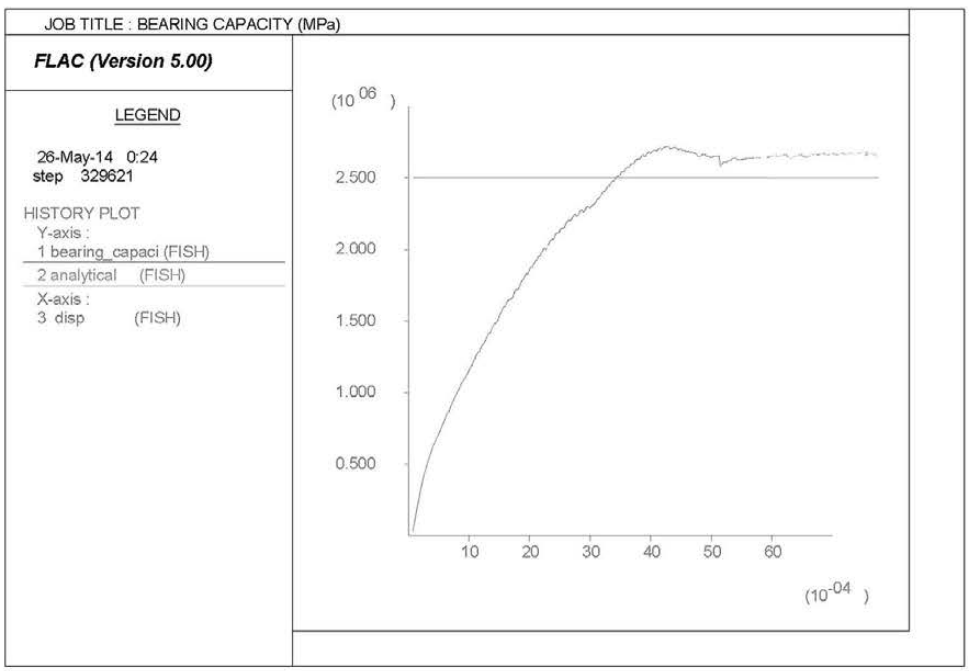

Fig. 6. History of load at the tip of a pile (load); analytical solution (sol) also shown for a plane model ($GSI=15$; $m_0=15$; $\sigma_c=2$ MPa; $\gamma_R=15$ kN/m^3; $H_R=0.8$ m; $B=0.8$ m; $H_s=6$ m; $\gamma_s=18$ kN/m^3).

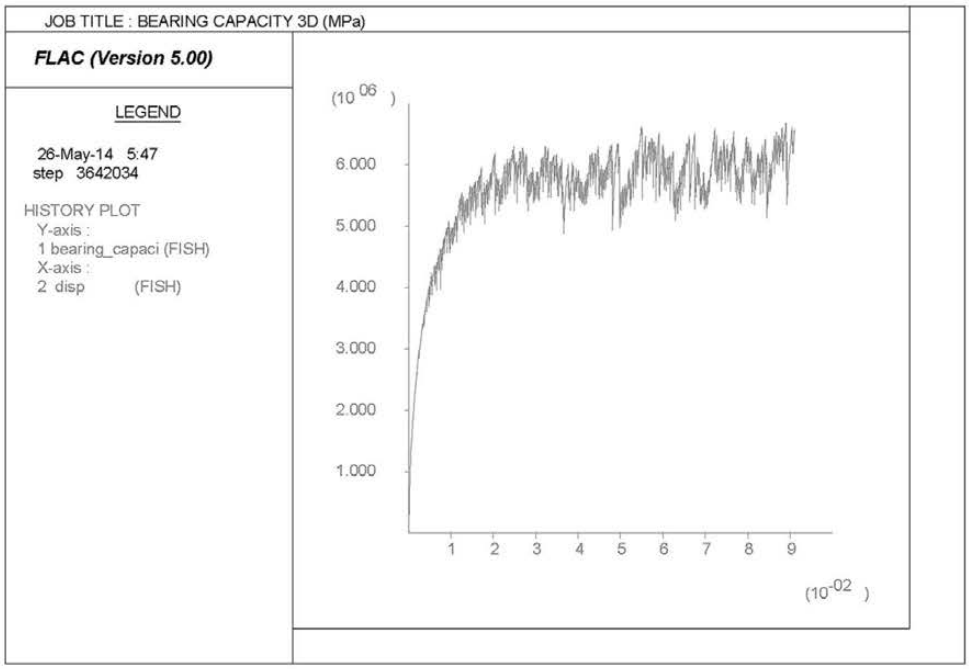

Fig. 7. History of load at the tip of a pile (load); analytical solution (sol) also shown for an axisymmetric model ($GSI=15$; $m_0=15$; $\sigma_c=2$ MPa; $\gamma_R=15$ kN/m^3; $H_R=0.8$ m; $B=0.8$ m; $H_s=6$ m; $\gamma_s=18$ kN/m^3).

geotechnical analysis software FLAC [9]. The analytical formulation presented in the previous sections is compared with the numerical solution obtained by the method of finite differences applied to developed examples in Section 5. Results of varying the uniaxial compressive strength of the matrix rock ($\sigma_c=2$ and 5 MPa) and parameter m_0 of the matrix rock ($m_0=7$ and 15) are also analyzed.

Adequate numerical model to validate the analytical solution should be initially a 2D model, as the obtained theoretical formulation is raised in plane strain. The analytical formulation allows to predict the three-dimensional bearing capacity using the shape factor developed by De Beer; therefore, also 3D numerical calculations are performed using axisymmetric models to validate whether this coefficient allows to obtain values on the safety side.

In the used numerical models (Fig. 5), the rock mass is discretized using an adaptive mesh and a constant velocity (small enough to prevent the development of inertia forces) is applied to the nodes of the mesh located at the tip of the pile. This velocity allows monitoring the implementation of an increasing burden solely on the support of the pile in the rock mass until reach the ultimate bearing capacity. Null horizontal displacement condition on the vertical walls of the rock mass which is in contact with the pile has been introduced. In addition, the soil layer is considered as overburden applied on top of the rock mass.

The results obtained of ultimate bearing capacity at the tip are briefly presented in Table 1, with a graphic output of the plane model (Fig. 6) and for axisymmetric model (Fig. 7) corresponding to one simple case. It is noted that very similar values are obtained from the proposed analytical solution and the numerical models results. It can also be noted that the factor of De Beer adopted for consideration of three-dimensional effect is on the safe side.

7. Conclusions

The modified Hoek–Brown criterion [3,6] has been used to calculate the ultimate bearing capacity at the tip of a pile embedded in a rock mass using the plasticity theory and the characteristics method, as was done in the previous paper [1] with the original Hoek–Brown criterion [2]. This procedure is valid under the assumptions of perfect plasticity, homogeneity, isotropy, weightless rock media, without inertia forces and Meyerhof's hypothesis [4]. Plane strain hypothesis is initially assumed and the shape factor developed by De Beer [5] is introduced later.

The modified Hoek–Brown criterion, assuming an associative flow law, formulated in principal stresses [Eq. (1)] can also be expressed in a mathematically rigorous manner using the classical shear (τ) and normal (σ) stresses (Mohr's envelope of the stresses) under parametric form depending exclusively on the instantaneous internal friction angle [Eqs. (12) and (13)]. These formulae are valid for determining the characteristic lines equations that govern the plasticity problem. Discriminant expression of two possible types of piles behavior according to the value of the acting overburden h_m is formulated. Eq. (35) indicates the actual embedment value, while expressions (38) and (39) allow to obtain the limit embedment values n_{L1} and n_{L2} for the cases of major and minor overburden.

The ultimate bearing capacity at the tip of a pile is calculated by means of Eq. (41) and previous ones. A new bearing capacity factor, $N_{\beta p}$, is formulated according to Eqs. (33) and (41). The shape coefficient, s_β, is calculated using friction angles acting in both boundaries as is indicated by Eq. (40).

The analytical solution obtained is compared with numerical models under plane strain, obtaining very close results in both cases. Also, an axisymmetric model is performed to check that the shape factor developed by De Beer is on the safety side. The entire formulation can be programmed in a spreadsheet.

References

Serrano A, Olalla C. Ultimate bearing capacity at the tip of a pile in rock, part I: theory. Int J Rock Mech Min Sci 2002;39:833–46.
Hoek E, Brown E. Empirical strength criterion for rock masses. J Geotech Eng Div Am Soc Civ Eng 1980;106(GT9):1013–35.
Hoek E, Wood D, Shah S. A modified Hoek–Brown criterion for jointed rock masses. In: Hudson JA, editor. Proceedings of the rock characterization

symposium of ISRM: Eurock 92. London: British Geotechnical Society; 1992. p. 209–24.
Meyerhof GG. The ultimate bearing capacity of foundations. Geotechnique 1951;II(4):301–21.
De Beer EE. Experimental determination of the shape factors and the bearing capacity factors of sand. Geotechnique 1970;20:387–411.
Hoek E, Carranza-Torres C, Corkum B. Hoek–Brown failure criterion – 2002 edition. In: Hammah R, Bawden W, Curran J, Telesnicki M, editors. Proceedings of NARMS-TAC, Toronto; 2002. p. 267–73.
Serrano A, Olalla C, Gonzalez J. Ultimate bearing capacity of rock masses based on the modified Hoek–Brown criterion. Int J Rock Mech Min Sci 2000;37: 1013–8.
Serrano A, Olalla C. Ultimate bearing capacity of rock masses. Int J Rock Mech Min Sci Geomech Abstr 1994;31:93–106.
Itasca Consulting Group, Inc FLAC, Fast lagrangian analysis of Continua, Version 5.0 Fluid-Mechanical Interaction. Minneapolis; 2005.